Turk J Phys
35 (2011) , 23 – 29.

doi:10.3906/fiz-1001-7

The low temperature resistivity of thermally evaporated antiferromagnetic Mn_{100-X} Ru_x thin films

Francis Kofi AMPONG and Francis BOAKYE
Department of Physics, Kwame Nkrumah University of Science and Technology, Kumasi-GHANA
e-mail: kampxx@yahoo.com

Received: 31.01.2010

Abstract

Electrical resistivity measurements on thermally evaporated Mn_{100-x} Ru_x thin films (with $x = 0.05$ at.% Ru and $x = 2.5$ at.% Ru) have been carried out over the temperature range from 300 to 1.4 K. A behaviour typical of the bulk α-Mn has been observed on the film with $x = 0.05$ at.% Ru. The Néel point of this specimen is established at 90 $\pm$ 1 K which is typical of the bulk. This Néel point is raised to 100 $\pm$ 1 K with $x = 2.5$ at.% Ru in α-Mn. A relatively long range magnetic ordering was observed with $x = 0.05$ at.% Ru in α-Mn indicating that the concentration of Ru has an adverse effect on antiferromagnetism in α-Mn. The low temperature resistivity of the 2.50 at.% Ru in α-Mn can be explained in terms of Kondo scattering.

Key Words: Resistivity, spin disorder scattering, kondo scattering

1. Introduction

Manganese appears in the seventh column of the periodic table in the middle of the first transition period. It is extremely anomalous even when compared with its neighbours in the first transition series, or with the corresponding members of the second and the third transition series. α-Mn has a cubic structure with lattice constant 8.91Å and contains 58 atoms per unit cell. Bradley and Thewlis [1] showed that the structure contained four crystallographically non-equivalent sites.

The basis of the whole arrangement is a simple body-centered-cubic lattice, with each lattice point being associated with a cluster of 29 atoms. Around each type-I atom is an octahedron of type-IV atoms, the opposite faces of the octahedron being of different sizes so that the symmetry is tetrahedral.

The four type-II atoms are somewhat further from the center of the group and are arranged tetrahedrally about the center. The twelve outer-most type-III atoms comprise a polyhedron having cubic and octahedral faces. The whole cluster has symmetry which is tetrahedral, as is that of the crystal as a whole.

$\alpha-$Mn is in many respects analogous to an intermetallic compound. As a matter of fact, an intermediate phase generally called the χ phase, has a structure isomorphous with α-Mn. This χ phase has been identified

in several binary and ternary alloys [2–5]. Two factors would appear to be in operation in stabilizing both α-Mn and the χ phase. They are electronic structure and atomic sizes.

The coordination numbers (CN) for the α-Mn sites are site-I, CN 16; site II, CN 16; site III, CN 13 and site IV, CN 12 [3]. There is a striking difference between interatomic distance within the Mn structure, as well as coordination numbers associated with the various sites. The interatomic distance vary from 2.21 to 2.96Å [3] and the coordination numbers vary from the impact icosahedral with CN12, to sites with CN16 which occupy considerable more volume. From consideration of space filling, it would appear that the Mn atoms, in sites I and II would tend to have a larger electronic radii in order to fill the relatively larger volume of the CN 16 sites. Smaller atoms on the other hand, would occupy the sites III and IV, since there is a smaller volume associated with the CN 13 and CN 12 sites. From size consideration, it might be expected that Mn exists in different electronic states.

Several neutron-diffraction studies of the magnetic structure have been carried out [6–9]. These studies have shown that each of the four non-equivalent atomic sites have different magnetic moments and established the existence of antiferromagnetic state in α-Mn below a temperature of approximately 95 K.

From consideration of atom sizes, predictions can be made with regards to the effects of alloying. One may expect atoms of relatively smaller sizes such as Cr and Fe, to preferentially occupy the smaller sites III and IV. On the other hand, relatively larger atoms such as Mo, Re and Ru might be expected to preferentially occupy the large sites, I and II. It has been shown [10, 11] that pure α-Mn exhibits a sharp cusp in its resistivity curve around 95K. William and Standford [12] noted that this temperature corresponds to the temperature at which antiferromagnetism sets in as reported in the Neutron diffraction studies. Thus this minimum is thought to be associated with the ordering temperature T_N. Coles [13] has suggested that each change in the resistance curve can be explained by the presence of a large spin-disorder resistance above the Néel temperature. Cooling through this temperature produces a reduction in the spin-disorder scattering and, at the same time, a change in the conduction-electron configuration. The temperature dependence and this resistivity anomaly depend on the amount and type of the impurities in the sample. Boakye [14] found that the addition of cobolt tends to raise the Néel point while the addition of Chromium tends to suppress it [15]. In this communication, we report on the resistivity temperature curves of $Mn_{100-x}Ru_x$ thermally evaporated thin films with $x = 0.05$ at.% Ru and $x = 2.50$ at.% Ru and their respective Néel points using the hydrodynamical transition given by Craig and Goldberg [16], and the anomalous low temperature-resistivity of these alloys.

2. Experimental details

The starting materials were 0.05 at.% Ru in Mn and 2.50 at.% Ru in Mn, all obtained from BDH chemicals Ltd., Poole, England. The purity of each component of the Mn-Ru alloy is quoted by the manufacturers as 99.998%. The films were prepared by thermal evaporation on to thin glass substrates cut to size and cleaned. Each alloy was first cleaned in 5% HCl in methanol to remove surface oxides and other contaminants. They were then dried and ground immediately before being loaded into a previously cleaned molybdenum boat. Since the components may evaporate at different rates because of their different vapour pressure, a flash evaporation (with a rate approximately 300 As^{-1}) was used for the two films from the two components used in these experiments. An AUTO 306 coating unit from Edwards High vacuum Ltd. was used in this operation. This unit has a radiant heater capable of maintaining substrate temperatures up to 350 °C. The substrates were thin glass slides which were cut into squares of side 8mm to fit into an α-brass mask designed to produce the required

film shape. The glass pieces which were to serve as substrates were cleaned in Genklene before being loaded in position in the mask. In these experiments, the substrates were held at 300 °C for each deposition. Substrate temperatures were measured with a copper constantan thermocouple incorporated with the unit. To achieve the correct substrate temperature, the hot junction of the thermocouple was screwed on the mask. Film thicknesses were measured with an interferometer and the ambient pressure in the bell jar was measured with an ion gauge incorporated into the unit. The ambient pressure was kept at 2×10^{-6} Torr for each specimen. To achieve this, the unit was pumped down for 8 hours for the two specimens. Resistivity measurements between 300 and 1.4 K were carried out by the van der Pauw four probe technique [17] in a conventional ^{4}He cryostat as described by Swallow [18]. Temperatures between 300 and 60 K were measured with a copper resistance thermometer. Below 60 K, the copper resistance thermometer was insensitive and a carbon resistance thermometer was used. This has a resistance of about 200 Ω at 25 K and rises to about 300 Ω at 4.2 K. This sensor is therefore extremely sensitive for temperatures below 4.2 K. In conjunction with this sensor, temperatures below 4.2 K were measured with a gas thermometer. These temperatures were deduced directly from ^{4}He vapour pressure with an accuracy of about 0.5%. Above about 2 K, the vapour pressure was measured with a mercury manometer and below 2 K it was measured with an oil manometer filled with low vapour pressure Apiezon 704 oil. The oil manometer was calibrated against the mercury manometer around about 2 K. Calibration checks were also made around these temperatures with the carbon resistance thermometer.

3. Results and discussion

3.1. Electrical resistivity of Mn-Ru alloys

Figure 1 illustrates the electrical resistivity of the Mn films with $x = 0.05$ and $x = 2.50$. Firstly, there is a gradual linear drop in resistivity in the two cases from 300 K. This behaviour is attributed to the phonon scattering of the conduction electrons [19]. In the case of $x = 0.05$ at.% Ru, the resistivity goes through a minimum at a temperature of 100 K before rising to a maximum at 70 K. The resistivity then falls sharply. This decrease in resistivity due to the magnetic ordering of the spins does not however give $\rho(0) = 0$ as would be expected in a pure and perfect specimen of a magnetic metal but rather tends to a higher value of 1.20 $\mu\Omega$m as compared with 0.81 $\mu\Omega$m of α-Mn film results of Boakye et al. [19–21].

In the case of the 2.50 at.% Ru, the resistivity minimum occurs at 120 K and goes through a maximum at 80 K. After the resistivity maximum, there is a relatively short range magnetic ordering and the resistivity goes through a minimum again at 36 K. The excessive scattering after the second minimum could be connected with the lattice distortion in the high Ru concentration alloy. Consequently, one may infer that the introduction of 0.05 at.% Ru into α-Mn does not affect anti ferromagnetic coupling by a simple dilution process. However, it is known that both magnetic and non magnetic disorder affect the magnetic and electrical properties of materials in several theoretical models [22].

3.2. The Néel point of Mn-Ru thin films

Williams and Stanford [12] have made an attempt to understand the nature of the complex magnetic interaction in antiferromagnetic α-Mn and its alloys by their studies in resistivity temperature curves. They define the Néel point as corresponding to the first minimum on the resistivity temperature curve. This is in contradiction with the magnetic scaling theory. Zumsteg and Parks [23] have defined the Néel point as that temperature at which the temperature dependent magnetic coherence length ξ approximately equals the phonon

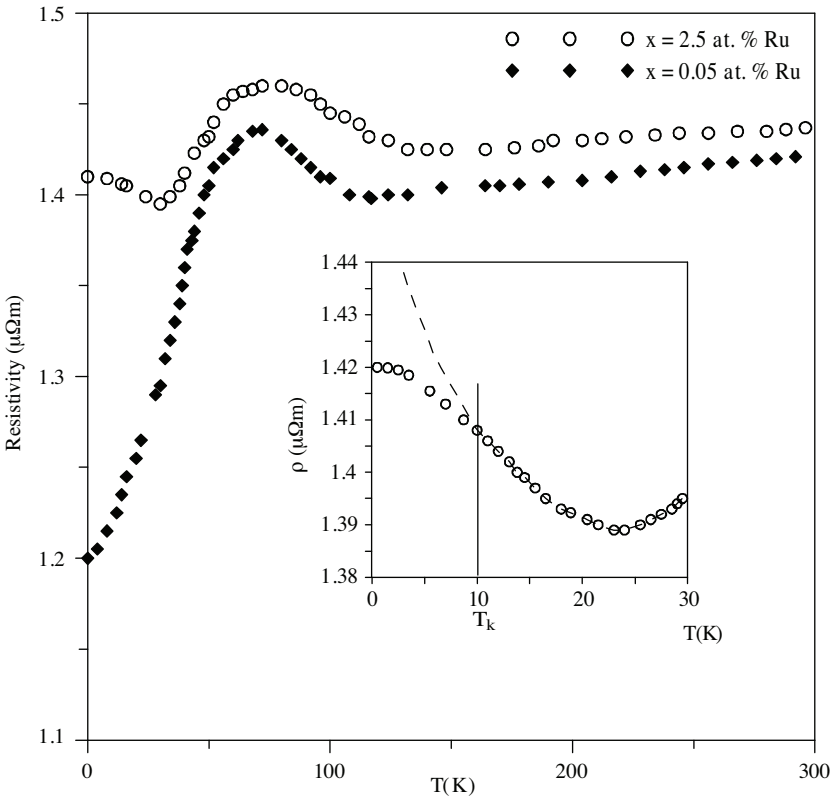

Figure 1. Resistivity as a function of Temperature for Mn thin films. (Open circles ◯ show data for $x = 2.5$ at.% Ru, black diamonds ♦ show data for $x = 0.05$ at.% Ru, and the inset show ρ as a function of T at low temperatures; the broken line indicates the Kondo in terms of $\ln T$.)

limited mean free path of the conduction electrons. Craig and Goldburg [16] have pointed out that the anomaly in the temperature derivative of the resistivity $\delta \mathrm{p}/\delta \mathrm{T}$ that gives a singularity marks the transition from the hydrodynamic regime to the critical regime predicted by the magnetic scaling theory and the anomaly is believed to lie in the strong temperature dependence of the phonon limited mean free path in the neighbourhood of the ordering temperature. This hydrodynamic-critical transition is defined by the position of the singularity in the temperature of the resistivity versus temperature. Consequently, a plot of the temperature derivative $\delta \mathrm{p}/\delta \mathrm{T}$ against temperature defines the Néel point T_N in antiferromagnetic materials. It is being suggested therefore that the claim by Williams and Standford [12] that the Néel point corresponds to the first resistivity minimum, could be considered as an onset of antiferromagnetic transition.

Figures 2 and 3 illustrate the case of $\delta \mathrm{p}/\delta \mathrm{T}$ as a function of T for 0.05 at.% Ru and 2.5 at.% Ru, respectively. In each case, it goes with an overlay of its resistivity-temperature curve. The results show that with the 0.05 at.% Ru in Mn, the Néel point is 90 ± 1 K whilst with the 2.5 at.% Ru, the Néel point is 100 ± 1 K, displaying a shift of 10 K to an upper value.

3.3. The low temperature resistivity minimum

The resistivity temperature behaviour of α-Mn at low temperatures is also of interest. Nagasawa and Semba [24] observed a coefficient of T^2 term upon the addition of 3d transition metal impurities. A change of

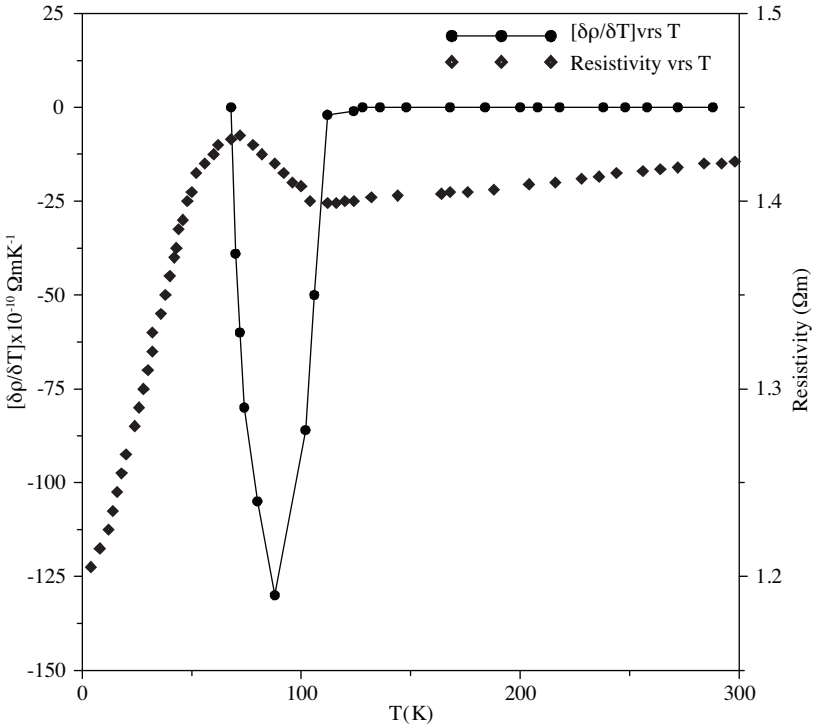

Figure 2. $\delta\rho/\delta t$ as a function of temperature for 0.05 at.% Ru (black circles, •) with an overlay of resistivity ρ as a function of temperature T (diamonds, ♦).

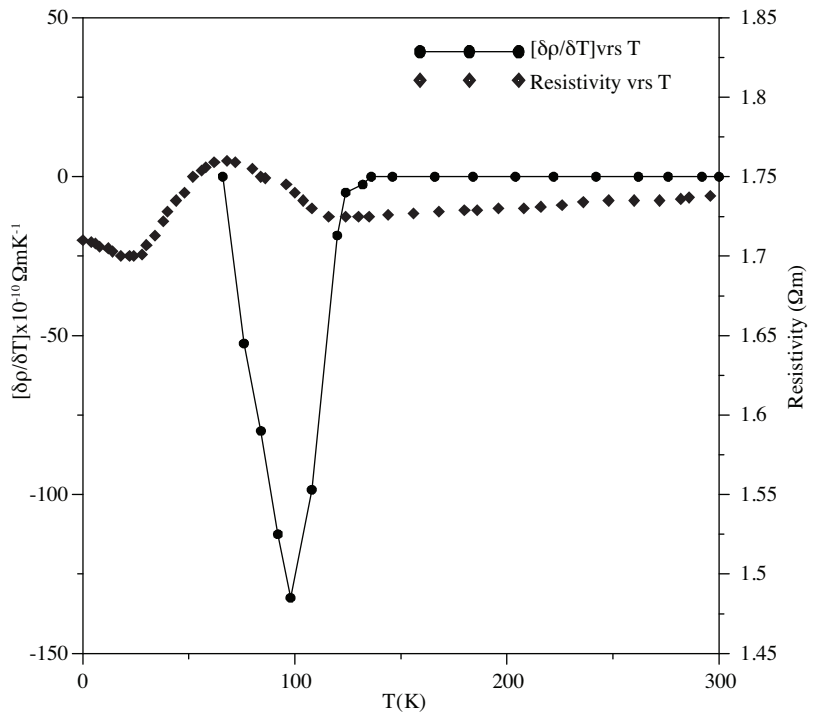

Figure 3. $\delta\rho/\delta$t as a function of temperature T for 2.5 at.% Ru (shown in black circles, •) with an overlay of resistivity ρ as a function of T (diamonds, ♦).

the sign of the coefficient and the low temperature resistivity minimum phenomenon were observed for alloys containing V, Co and Ni impurities. This has been confirmed by Boakye in his recent paper on antiferromagnetic transition in thermally evaporated Manganese-Vanadium alloys [25]. Electrical resistivity studies of thermally evaporated manganese-rhenium thin films by Boakye [26] has revealed that the low temperature resistivity in some of these alloys might be due to Kondo scattering. This is the feature being displayed by the 2.5 at.% Ru in α-Mn.

Kondo [27] has given a theory which provides valuable information in understanding the low temperature resistivity minimum of these alloys. He found that the resistivity ρ can be given in the expression

$$\rho = \rho_{phon} + c\rho_A + c\rho_m + c(3ZJ\rho_m/E_f)\ln T,$$

where ρ_{phon} is the phonon resistivity, c is the impurity concentration, ρ_A the resistivity per concentration due to the impurity potential, ρ_m a temperature-independent quantity occurring in the expression for the spin scattering resistivity, Z the number of conduction electrons per atom, E_f is the Fermi energy and J denotes the exchange constant for the interaction between the localized d-electrons and the conduction electrons. The value of J may be negative and in this case the last term in the expression will increase as the temperature is reduced. The logarithmic Kondo term is dependent on the concentration of the solute and this might be responsible for the shift of T_N since this term affects the $\rho(T)$ pattern. Figure 1 illustrates the resistivity-temperature curves of the two specimens revealing the low temperature behaviour of the specimens as T approaches zero. In order to extract the Kondo temperature T_K, it is necessary to do a $\ln T$ curve fitting as illustrated in Hurd [28]. T_K is established at 10 K for our 2.5 at.% Ru, as shown on the inset of Figure 1. The logarithmic Kondo term therefore explains the divergence of the resistivity of this particular sample as T approaches zero. It therefore appears that the magnitude of c influences the shift of the Néel point to a higher value.

4. Conclusion

Behaviour typical of the bulk α-Mn has been observed on the film $x = 0.05$ at.% Ru with a Néel point located at 90 $\pm$ 1 K. This Néel point is raised to 100 $\pm$ 1 K with $x = 2.5$ at.% Ru in α-Mn. A relatively long range magnetic ordering is observed with $x = 0.05$ at.% Ru in α Mn indicating that the concentration of Ru has an adverse effect on antiferromagnetism in α-Mn. The low temperature resistivity of the 2.5 at.% Ru in α-Mn can be explained in terms of Kondo scattering.

References

[1] A. J. Bradley and J. Thewlis, *Proc R. Soc.*, **AU5**, (1927), 456.

[2] M. V. Nevitt, *in Electronic structure and Alloy Chemistry of Transition Metals*, ed. by Beck, (Interscience, New York. 1963) p. 101.

[3] J. S. Kasper, *Theory of Alloy Phases* (American Society of Metals, Cleveland, Ohio, 1956) p. 264.

[4] C. W. Kimball, W. C Philips, M. V. Nevitt and R. S. Preston, *Phys. Rev.*, **146**, (1966), 375.

[5] J. S. Kasper, *Acta Mater.*, **2**, (1954), 456.

[6] G. G. Shull and M. K. Wilkinson, *Rev. Mod. Phys.*, **25**, (1956), 100.

[7] J. S. Kasper and B. W. Roberts, *Phys. Rev.*, **101**, (1956), 537.

[8] J. A. Oberteuffer, J. A. Marcus, L. H. Schwartz and G. P. Felcher, *Phys Rev.*, **B2**, (1970), 670.

[9] T. Yamada, N. Kunitomi, Y. Nakai, D. E. Cox and G. Shrine, *J. Phys. Soc. Jpn.*, **28**, (1970), 28.

[10] R. V. Bellau and B. R. Coles, *Proc. Phys. Soc. Lond.*, **82**, (1963), 121.

[11] G. T. Meadeau and P. Pelloux-Gervais, *cryogenics.*, **5**, (1965), 227.

[12] W. Williams Jr. and J. L. Stanford, *Phys. Rev.*, **B7**, (1973), 3244.

[13] B. R. Coles, *Adv. Phys.*, **7**, (1958), 40.

[14] F. Boakye and K. G. Adanu, *Cryogenic.,* **39**, (1999), 933.

[15] P. P. Craig and W. I. Godburg, *J. Appl. Phys.*, **40**, (1969), 964.

[16] L. J. Van der Pauw, *Philips Res. Rep.,* **1**, (1958), 13.

[17] G. A Swallow, Ph.D thesis University of Sussex, UK, 1968.

[18] F. Boakye and A. D. C. Grassie, *Thin Solid Films.,* **221**, (1992), 224.

[19] F. Boakye, K. G. Adanu and A. D. C. Grassie, *Mater Let.,* **18**, (1994), 320.

[20] F. Boakye and K. G. Adanu, *Thin Solid Films.,* **279**, (1996), 224.

[21] R. K. Nkum and F. Boakye, *Turk. J. Phy.*, **24**, (2000), 681.

[22] F. C. Zunsteg and H. D. Parks, *Phys Lett.*, **24**, (1974), 520.

[23] H. Nagasawa and M. Semba, *J. Phy. Soc. Jpn.*, **34**, (1975), 70.

[24] F. Boakye, *Turk. J. Phys.,* **31**, (2007), 51.

[25] F. Boakye, *Cryogenics.*, **43**, (1964), 37.

[26] J. Kondo, *Progr. Theor. Phys.*, **32**, (1964), 37.

[27] C. M. Hurd, *Electrons in Metals,* (New York. 1975) p. 187.